Failure Modes of Sand in Undrained Cyclic Loading: Impact of Sample Preparation

H. Y. Sze, A.M.ASCE[1]; and J. Yang, F.ASCE[2]

Abstract: This paper presents a systematic experimental investigation into the impact of specimen preparation on the cyclic loading behavior of saturated sand, including the deformation pattern, pore-water pressure generation, stress-strain relationship, and cyclic shear strength. Moist tamping and dry deposition were used in the laboratory to prepare sand specimens with distinct fabrics for cyclic triaxial tests under a range of conditions. It is found that the soil fabric formed by dry deposition can lead to unique failure modes different from those of moist-tamped samples in certain situations. These failure modes are hybrid in nature, characterized by a contractive response in the form of limited flow followed by cyclic strain hardening in the form of either cyclic mobility or plastic-strain accumulation. The hybrid nature of the failure patterns makes defining failure for liquefaction-resistance evaluation crucial; the conventional failure criteria based on a certain level of strain or pore-water pressure do not appear to properly represent the failure mechanism involved and may lead to a substantial overestimation of liquefaction resistance. The experiments reveal that the method used to reconstitute specimens or the soil fabric they form plays a role that is far more complicated than previously thought. Depending on the combination of relative density, confining stress, and degree of stress reversal in cyclic loading, a change of reconstitution method can have a marked or little effect on the nature of the response in terms of deformation pattern and failure mechanism; nevertheless, the two reconstitution methods always give significantly different liquefaction-resistance values under otherwise similar testing conditions. **DOI: 10.1061/(ASCE)GT.1943-5606.0000971.** *© 2014 American Society of Civil Engineers.*

Author keywords: Cyclic strength; Failure; Laboratory tests; Soil liquefaction; Soil fabric; Sand (soil type).

Introduction

Laboratory observations have consistently found that two specimens of a sand prepared by different reconstitution methods to the same density may display quite different responses to applied monotonic loading under otherwise similar conditions (e.g., Arthur and Menzies 1972; Oda 1972; Miura and Toki 1982; Vaid et al. 1999; Yang et al. 2008). The differences are thought to be linked to the different fabrics of the specimens formed by the different methods, which can be defined as the spatial arrangement of sand particles and associated voids (Brewer 1964; Oda and Iwashita 1999). How to take fabric effects into account in geotechnical analysis remains a difficult problem that attracts efforts on both theoretical and practical levels. A recent attempt was made by Yang et al. (2008), who measured soil fabrics introduced by moist tamping and dry deposition, two commonly used methods for laboratory preparation of sand specimens (Ishihara 1993), and then introduced the measurements into a constitutive framework to model the monotonic behavior of sand.

When loading is cyclic rather than monotonic, the problem becomes more difficult. A number of experimental studies (e.g., Ladd 1974; Mulilis et al. 1977; Tatsuoka et al. 1986a; Yamashita and Toki 1993) have produced valuable data showing that the liquefaction resistance of saturated sand specimens remolded by different compaction procedures to the same density can be significantly different. For example, Mulilis et al. (1977) conducted a series of stress-controlled cyclic triaxial tests and found that sand specimens prepared by moist tamping exhibited a much higher resistance to liquefaction than their counterparts formed by air pluviation, with the liquefaction resistance of the specimens formed by water pluviation being in between.

Most of the previous studies tended to concentrate on the liquefaction resistance, also known as cyclic strength, defined as the relationship between the cyclic stress ratio (i.e., cyclic deviatoric stress divided by twice the initial effective confining stress) and the number of loading cycles required to cause liquefaction. However, investigation has been lacking into the fundamental aspects of cyclic behavior, such as how the method of sample preparation affects the nature and characteristics of the cyclic response of sand, including the deformation pattern, pore-water pressure generation, effective stress path, and stress-strain relationship. Such investigation is needed because it can provide useful insights into cyclic behavior as affected by soil fabric and is also of value to the development of constitutive models for the fabric effect.

Moreover, previous studies focused mainly on cyclic tests on isotropically consolidated specimens at a dense or medium-dense state. This means that cyclic loading was symmetrical about the hydrostatic axis with full stress reversal, and cyclic mobility would be the dominant failure pattern. Compared with isotropically consolidated specimens, anisotropically consolidated specimens may exhibit, under otherwise similar conditions, significant differences in both cyclic strength and response characteristics (e.g., Vaid and Chern 1983; Mohamad and Dobry 1986; Hyodo et al. 1994; Yang and Sze 2011a). Anisotropic consolidation has been used in the laboratory to investigate the effect of initial shear stress existing in dams, embankments, and slopes (Seed 1983; Idriss and Boulanger 2008).

[1]Formerly, Ph.D. Student, Dept. of Civil Engineering, Univ. of Hong Kong, Pokfulam, Hong Kong, China.

[2]Associate Professor, Dept. of Civil Engineering, Univ. of Hong Kong, Pokfulam, Hong Kong, China (corresponding author). E-mail: junyang@hku.hk

152 / JOURNAL OF GEOTECHNICAL AND GEOENVIRONMENTAL ENGINEERING © ASCE / JANUARY 2014

J. Geotech. Geoenviron. Eng. 2014.140:152-169.

The presence of an initial shear stress leads to cyclic loading that is nonsymmetrical about the hydrostatic state with or without partial stress reversal, which can result in different failure modes in certain situations (Yang and Sze 2011a). In this context, careful examination is needed of the impact of the reconstitution method under this nonsymmetrical cyclic-loading condition.

This paper presents an experimental study aimed at investigating in a systematic way the impact of specimen preparation on the cyclic behavior of saturated sand, covering both symmetrical and non-symmetrical loading conditions. Moist tamping and dry deposition were used in this study to prepare specimens with distinct fabrics. As evidenced by the microscopic measurements of Yang et al. (2008), the dry-deposition method is able to produce specimens that are an-isotropic, whereas moist-tamped specimens are generally isotropic. For either reconstitution method, three initial state parameters—density, mean confining stress, and static shear stress—were systematically varied over a broad range. As will be seen later, this strategy is important because it allows one to isolate the effect of each parameter from the other two and at the same time investigate their interdependency. To facilitate identification of the effect of the reconstitution method, the initial testing conditions for specimens formed by the two methods were made essentially identical in terms of the three initial state parameters. In this paper, extensive test series are examined, interpreted, and com-pared, focusing on the cyclic deformation pattern, pore-water pressure buildup, cyclic-stress path, failure-criterion definition, and liquefaction-resistance evaluation. A grain-level explanation is also put forward to provide a better understanding of the various macroscopic observations.

Experimentation

Test Material and Equipment

The test material was Toyoura sand, a uniformly graded quartz sand with subangular grains. The sand has a mean particle size D_{50} of 0.216 mm and a uniformity coefficient of 1.392, with 0% fines content. Table 1 summarizes its basic properties. All tests were performed using an automated triaxial testing system, which is capable of performing a variety of functions, including isotropic and anisotropic consolidation and various modes of shear loading.

Specimen Preparation

The procedures of the moist-tamping (MT) and dry-deposition (DD) methods are briefly described in the following paragraphs, and schematic illustrations are presented in Fig. 1.

MT Method
Moist sand, mixed at 5% moisture content, was compacted in five layers to form a specimen that was 71.1 mm in diameter and 142.2 mm in height [Fig. 1(a)]. The undercompaction technique was employed to ensure sample uniformity by targeting the center layer at the desired initial density D_{ri}, with each successive lower and upper layer at 1% more or less, respectively. The MT method is able to produce a wide range of initial densities from an extremely loose to dense state.

DD Method
Oven-dried sand at a predetermined mass was deposited using a funnel into a split mold [Fig. 1(b)]. The funnel tip was maintained

Table 1. Basic Properties of Test Material

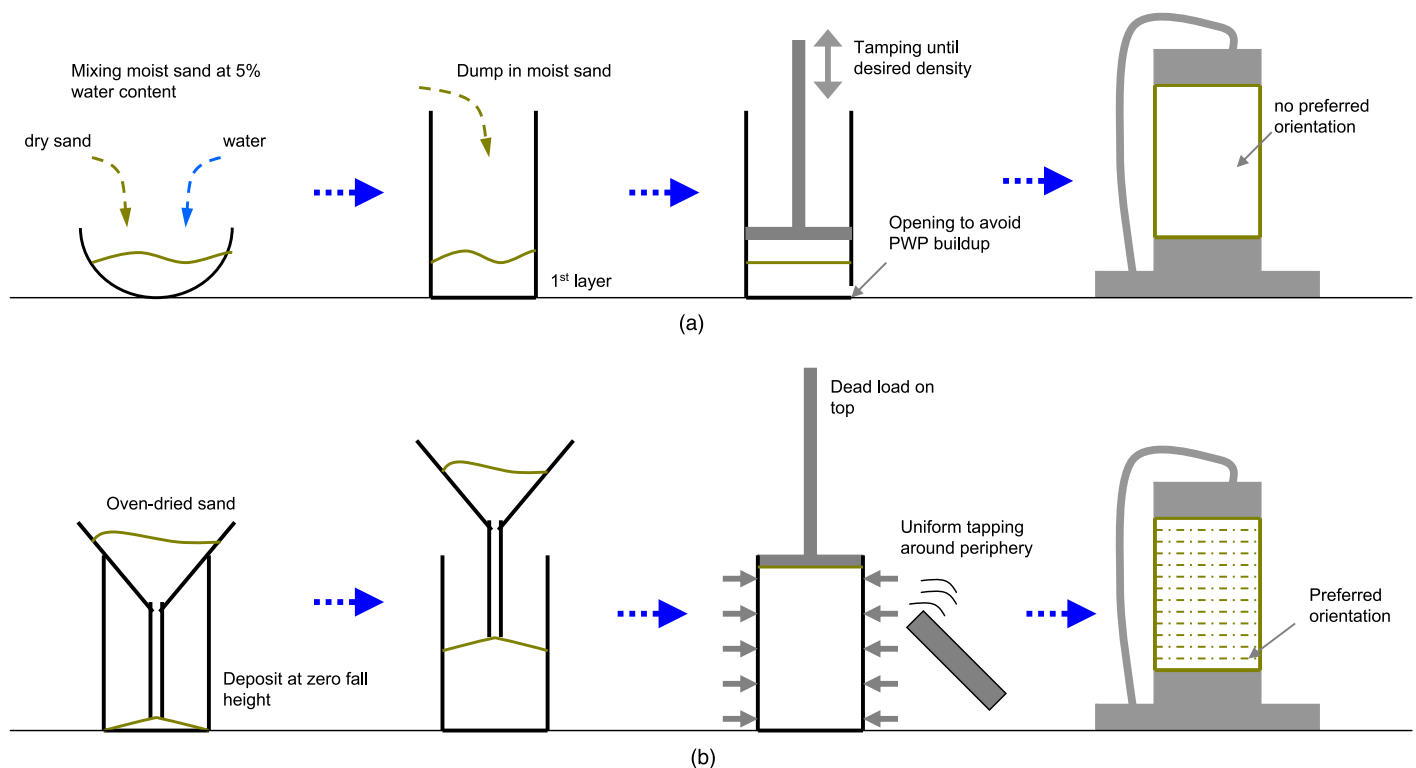| Mean particle size D_{50}	Coefficient of uniformity	Specific gravity	Maximum void ratio e_{max}	Minimum void ratio e_{min}	Fines content
0.216 mm	1.392	2.64	0.977	0.605	0%

Fig. 1. Schematic illustration of (a) MT and (b) DD methods for sample preparation

at a minimal height of drop above the sand's surface throughout so as to give the lowest possible density. Tapping was then done uniformly around the periphery of the mold using a rubber rod to achieve a higher density. As commented by Ishihara (1993), using DD to form uniform samples at a very loose state is hard. In this study, the lowest possible postconsolidation relative density D_{rc} was 20%, as compared with $\sim$10% using MT. DD is somewhat different from the method known as air pluviation (Tatsuoka et al. 1986a; Mulilis et al. 1977) in that the latter method involves pouring dry sand in air from a nozzle at a certain rather than zero height into a mold. Nevertheless, both methods share a similar principle that is distinctly different from that of MT.

Saturation and Consolidation

Each specimen formed by either the MT or DD method was brought to initial saturation through CO_2 flushing and then deaired water flushing, which was then followed by back-pressure saturation to achieve a B-value of greater than 0.98. On initial saturation, the specimen's dimensions were remeasured to ensure a better control of the density. In doing this, the specimen was mounted on the base pedestal of the triaxial cell with its top cap connected to a fixed point. Anisotropic consolidation was conducted under the major and minor principal stresses σ'_{1c} and σ'_{3c} to give rise to a static shear stress on the plane of maximum shear stress in the soil sample. The initial stress state in terms of the effective normal stress σ'_{nc} and the initial shear-stress ratio α are thus given as (Yang and Sze 2011a)

$$\sigma'_{nc} = \frac{\sigma'_{1c} + \sigma'_{3c}}{2} \qquad (1)$$

$$\alpha = \frac{q_s}{2\sigma'_{nc}} = \frac{\sigma'_{1c} - \sigma'_{3c}}{\sigma'_{1c} + \sigma'_{3c}} \qquad (2)$$

where q_s = initial deviatoric stress. Here σ'_{nc} rather than σ'_{3c} is used because it is the normal effective stress σ'_{nc} and the static shear stress $q_s/2$ on the 45° plane that simulate the field stress conditions (Seed and Lee 1966). The parameter α indicates the level of initial shear stress, with $\alpha = 0$ representing the special case where the initial shear stress is absent (i.e., isotropic consolidation).

The void ratio of each specimen at the end of consolidation was determined from the void ratio of the specimen measured before consolidation and the volumetric strain that the specimen underwent during consolidation. A different method was also used to estimate the postconsolidation void ratio by measuring the moisture content of the specimen after completion of the test (Verdugo and Ishihara 1996), and it was found that both methods gave consistent estimates. This consistency was also obtained by Yang and Wei (2012) in testing silty sands. However, when testing loose silty sand specimens that are highly compressible, more care is required in determining the void ratio, and the method of measuring moisture content is recommended (Yang and Wei 2012).

Cyclic tests were conducted under a stress-controlled, undrained condition, with cyclic loading characterized by the cyclic stress ratio CSR_n as

$$CSR_n = \frac{q_{\text{cyc}}}{2\sigma'_{nc}} \qquad (3)$$

where q_{cyc} = cyclic deviatoric stress. The loading was applied at a low frequency (0.01 Hz) to have stable input and output signals and thus reliable records of the response. Several previous studies have examined the frequency effect in cyclic loading tests and found that

this effect is insignificant (e.g., Peacock and Seed 1968; Wong et al. 1975; Tatsuoka et al. 1986b).

Test Series

Cyclic triaxial tests were conducted on specimens formed by MT and DD for a wide range of soil densities, mean confining stresses, and initial shear stresses. The purpose was to produce a systematic database of large size to allow a detailed examination of the interdependency of various factors and meanwhile to serve as a useful reference for the development of advanced constitutive models. Table 2 summarizes the test series for this purpose, which consists of more than 120 tests.

Deformation Patterns and Failure Mechanisms

Typical responses of the specimens prepared by DD and MT at similar testing conditions are examined in this section. For clarity, the discussion is organized according to the relative densities of the specimens after consolidation, ranging from a loose ($\sim$20%), to medium dense ($\sim$50%), and finally to dense state ($\sim$70%). As will be shown later, testing under a wide range of densities and for both $\alpha = 0$ and $\alpha \neq 0$ conditions is crucial for discovering the state dependence of the effect of the specimen preparation method.

Table 2. Test Series

Series	D_{rc} (%)	σ'_{nc} (kPa)	σ'_{3c} (kPa)	q_s (kPa)	a	Reconstitution method
I	20	100	100	0	0	MT, DD
	20	100	90	20	0.1	MT, DD
	20	100	85	30	0.15	DD
	20	100	75	50	0.25	MT, DD
	20	100	60	80	0.4	MT, DD
	20	100	40	120	0.6	MT
	20	500	500	0	0	MT, DD
	20	500	475	50	0.05	MT
	20	500	450	100	0.1	MT, DD
	20	500	375	250	0.25	MT, DD
	20	500	300	400	0.4	MT
II	35	100	100	0	0	MT, DD
	35	100	75	50	0.25	DD
	35	100	60	80	0.4	MT, DD
	35	100	50	100	0.5	MT, DD
	35	500	500	0	0	MT, DD
	35	500	450	100	0.1	MT, DD
	35	500	375	250	0.25	MT, DD
	35	500	300	400	0.4	MT, DD
III	50	100	100	0	0	MT, DD
	50	100	90	20	0.1	MT, DD
	50	100	60	80	0.4	MT, DD
	50	500	500	0	0	MT, DD
	50	500	375	250	0.25	DD
	50	500	300	400	0.4	MT, DD
IV	70	100	100	0	0	MT, DD
	70	100	90	20	0.1	MT, DD
	70	100	60	80	0.4	MT, DD

Note: MT = moist tamping; DD = dry deposition.

Effect on Behavior of Loose Samples

Fig. 2(a) shows the response of a specimen formed by DD, consolidated at a relative density of 20% and an effective confining stress of 500 kPa, and subjected to cyclic loading at $\alpha = 0$ and $q_{cyc} = 100$ kPa. The specimen did not exhibit notable axial deformation until at the 11th cycle of loading, when an excessive strain occurred suddenly. The triggering of this abrupt deformation was associated with a rapid buildup of excess pore-water pressure (PWP) straight to the level of effective consolidation stress, resulting in a total loss of strength of the sample. Prior to the onset of deformation, however, the PWP increased in a gradual manner. This failure mode is in many aspects the same with the flow-type failure observed in loose Toyoura sand samples formed by MT. To make this point clearly, Fig. 2(b) shows the response of an MT specimen at the same initial state and subjected to the same cyclic loading. Although a large difference in the number of cycles to failure is observed—this is related to liquefaction resistance, as will be discussed in detail later—the fabric difference introduced by the different sample preparation methods does not seem to have any appreciable effect on the deformation pattern. This is an interesting observation, but does it hold true for nonsymmetrical loading conditions?

The answer to this question is shown in Fig. 3, where the loading responses of a DD specimen and an MT specimen at the same initial state ($D_{rc} = 20\%$ and $\sigma'_{nc} = 500$ kPa) are presented in parallel. For both specimens, anisotropic consolidation was conducted in exactly the same way to give the same initial shear stress level ($\alpha = 0.1$), and a cyclic deviatoric stress of the same level (110 kPa) was then applied to give slight stress reversal. It is striking that although the level of the initial shear stress was not high, it was able to cause substantial behavioral differences. The loose specimen formed by DD did not undergo the flow-type failure with runaway deformation as in the absence of initial shear stress; rather, it exhibited somehow a limited-flow mode that is characterized by abrupt yet limited axial straining. The triggering of this limited flow occurred in the 12th cycle of loading. Note that at this instant the PWP also rose rapidly.

The term limited flow is used here because the mechanics of this failure mode appeared similar to that of flow-type failure in several
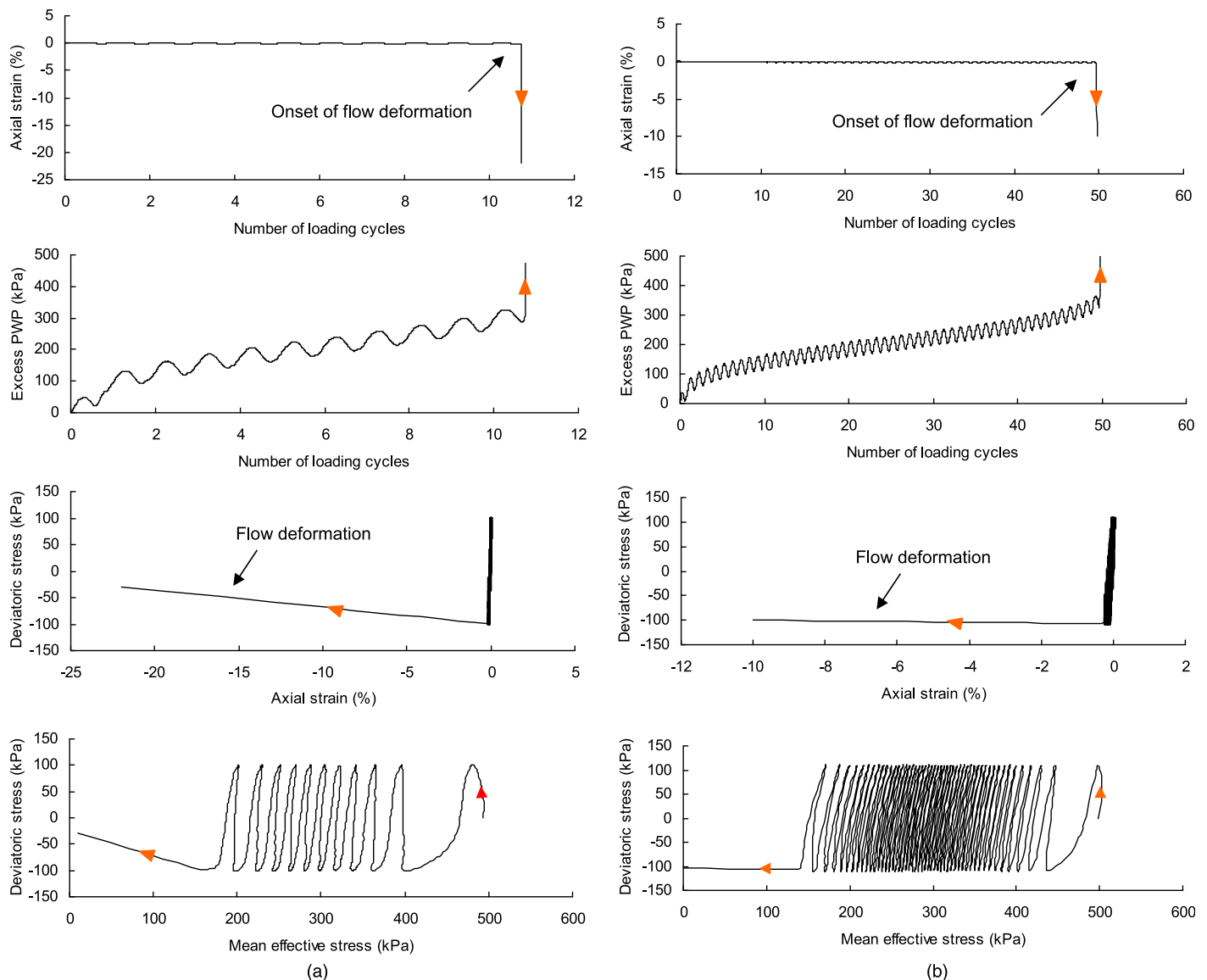

Fig. 2. Undrained response of loose sand specimens as a result of cyclic loading without presence of initial static shear ($D_{rc} = 20\%$, $\sigma'_{nc} = 500$ kPa, $\alpha = 0$): (a) DD specimen; (b) MT specimen
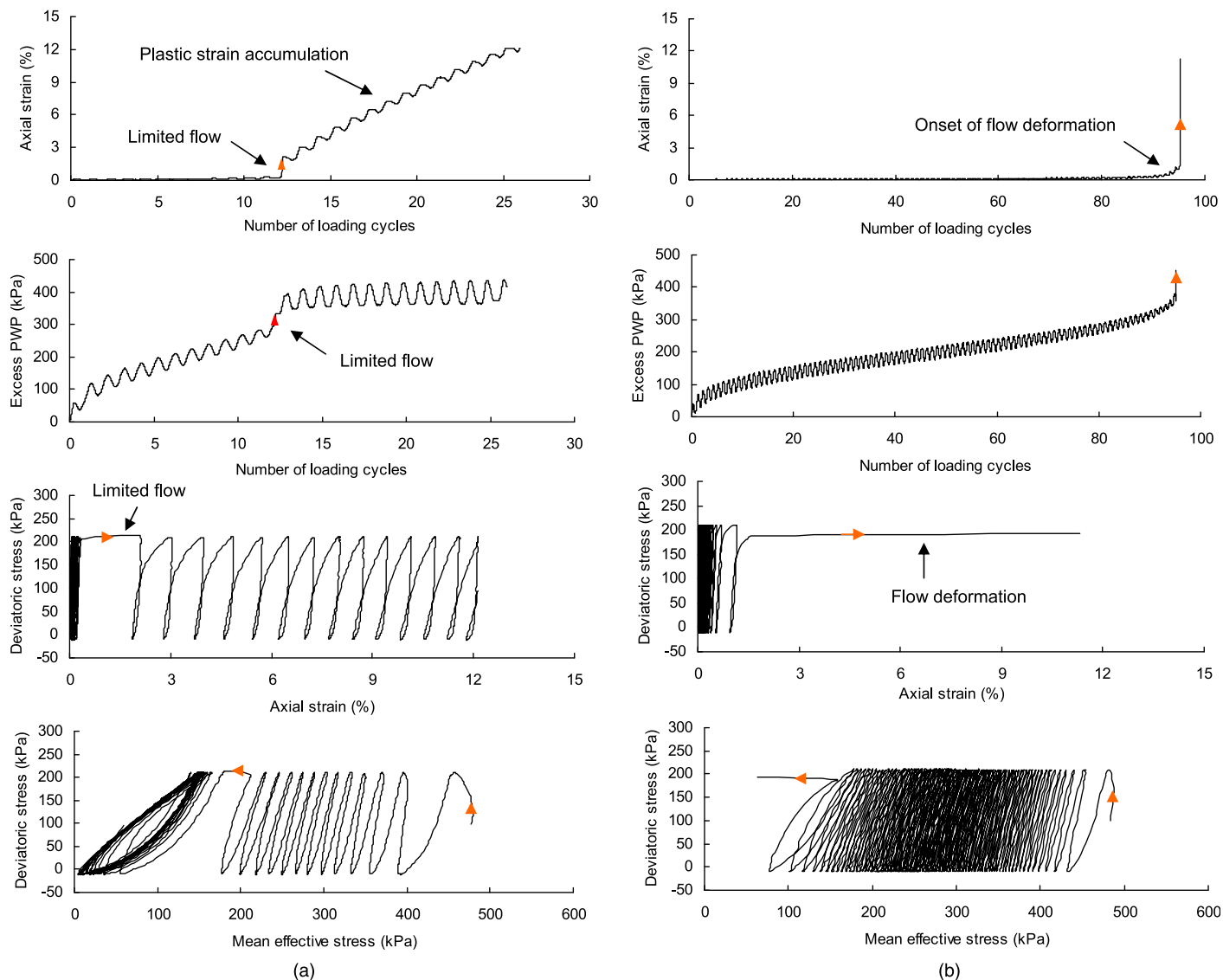
Fig. 3. Undrained response of loose sand specimens as a result of cyclic loading with presence of initial static shear ($D_{rc} = 20\%$, $\sigma'_{nc} = 500\,\text{kPa}$, $\alpha = 0.1$): (a) DD specimen; (b) MT specimen

ways, but the sample did not develop excessive deformations leading to complete loss of strength. Compared with the strain level of ~20% in flow-type failure [Fig. 2(a)], the resulting axial strain was less than 2%, which was immediately followed by plastic-strain accumulation at a rate of about 1% per loading cycle. Whereas the plastic strain accumulated at a fast rate, the PWP generation was quite steady. In terms of the stress path in the q-p' plane [$q = \sigma'_1 - \sigma'_3$ is deviatoric stress, and $p' = (\sigma'_1 + 2\sigma'_3)/3$ is mean effective stress], the behavior was obviously a hybrid failure mode combining both contractive and dilative responses. Also, the DD specimen failed on the compression side rather than on the extension side as in the absence of initial static shear [Fig. 3(a) versus Fig. 2(a)]; this result is reasonable because, given the initial static shear stress, the cyclic loading was dominated by compression.

As far as the test on the MT specimen is concerned, the presence of an initial shear stress of the same level does not seem to change the response characteristics or the deformation pattern [Fig. 3(b)]. The specimen still displayed the mode of flow-type failure except that excessive deformations occurred on the compression side in this case; this was due, again, to a lack of stress reversal.

The limited-flow mode observed in this study is similar to the so-called flow-deformation (Hyodo et al. 1994) and limited-liquefaction (Vaid and Chern 1985) patterns in the literature. However, in these previous studies, the effect of soil fabric was not recognized. A careful examination of these studies shows, coincidently and surprisingly, that either DD or air pluviation was used for sample reconstitution in their experiments. Note that DD and air pluviation are similar in principle and are expected to produce similar soil fabrics. This provides an important implication that the limited-flow mode is uniquely linked with the fabric formed by DD or air pluviation.

From the preceding discussion, a significant finding thus can be made that the sample preparation method shows different impacts under symmetrical and nonsymmetrical cyclic loading conditions. When an initial static shear stress is not present such that cyclic loading is symmetrical, the fabric difference brought about by different reconstitution methods does not have a marked effect on the failure mode; when an initial static shear stress is present such that there is no or only slight stress reversal in cyclic loading, the fabric difference can have a marked impact on the deformation pattern and
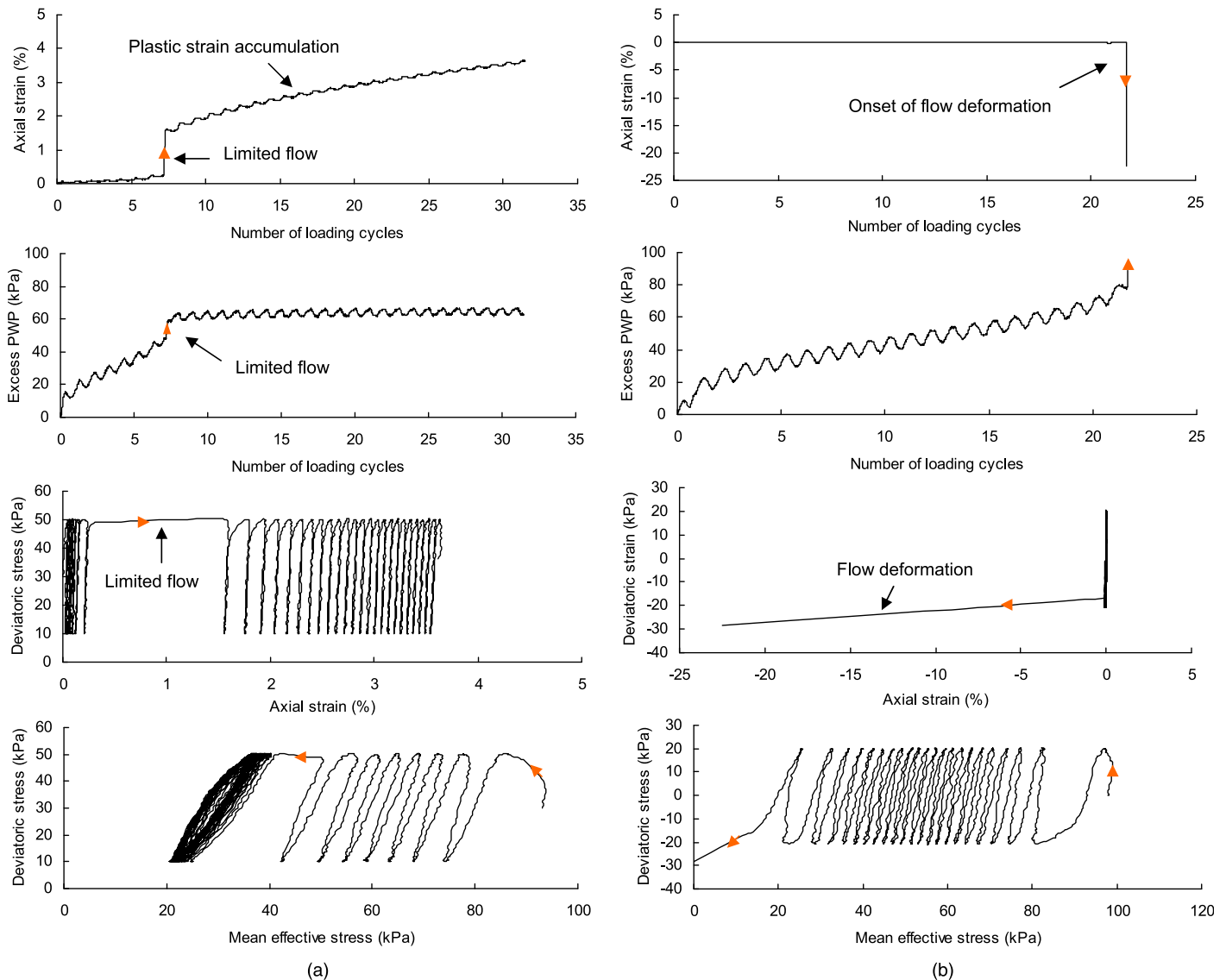
Fig. 4. Undrained response of loose sand specimens prepared by dry deposition as a result of cyclic loading ($D_{rc} = 20\%$, $\sigma'_{nc} = 100\,\text{kPa}$): (a) with initial shear ($\alpha = 0.15$); (b) without initial shear ($\alpha = 0$)

failure mechanism. To confirm this finding, two additional specimens were prepared by DD at a loose state ($D_{rc} = 20\%$ and $\sigma'_{nc} = 100\,\text{kPa}$). One specimen was subjected to a cyclic deviatoric stress in the absence of initial shear stress, and the other had a cyclic deviatoric stress of the same magnitude applied to it but with $\alpha = 0.15$. The results are compared in Fig. 4. As expected, the specimen cyclically loaded with an initial shear stress exhibited the limited-flow pattern, whereas the specimen under symmetrical loading displayed the flow-type mode.

Effect on Behavior of Medium-Dense Samples

Fig. 5(a) shows the response of a medium-dense specimen, prepared by DD and consolidated at $D_{rc} = 50\%$ and $\sigma'_{nc} = 100\,\text{kPa}$, under the symmetrical loading condition (i.e., $\alpha = 0$). Here another form of limited flow is discovered: an abrupt strain development ($\sim 3\%$) occurred in the 10th loading cycle and then was followed by a deformation pattern similar to cyclic mobility frequently observed in MT samples at a medium-dense state. To facilitate comparisons,

Fig. 5(b) presents the response of an MT specimen at the same initial state and subjected to symmetrically cyclic loading as well. Obviously, it was typical of the response known as cyclic mobility (Castro 1975). While being similar, the DD specimen did behave differently from the MT specimen in several aspects: (1) At the abrupt onset of deformations, the DD specimen developed quite a large strain in extension, whereas the MT specimen developed deformations in a progressive manner; and (2) the PWP in the DD specimen at the onset of deformations also underwent a big rise, leading to transient softening as recorded in the stress-strain curve and the stress path [Fig. 5(a)], whereas in the MT specimen the buildup of PWP was in a progressive manner throughout.

To confirm these interesting observations, another pair of specimens formed by DD and MT was isotropically consolidated to the same density but to a higher confining pressure ($\sigma'_{nc} = 500\,\text{kPa}$) and then were subjected to cyclic loading. The results are shown in Fig. 6. Again, the MT specimen was found to develop a typical cyclic-mobility response, whereas the DD specimen exhibited the limited-flow pattern characterized by a substantial yet limited
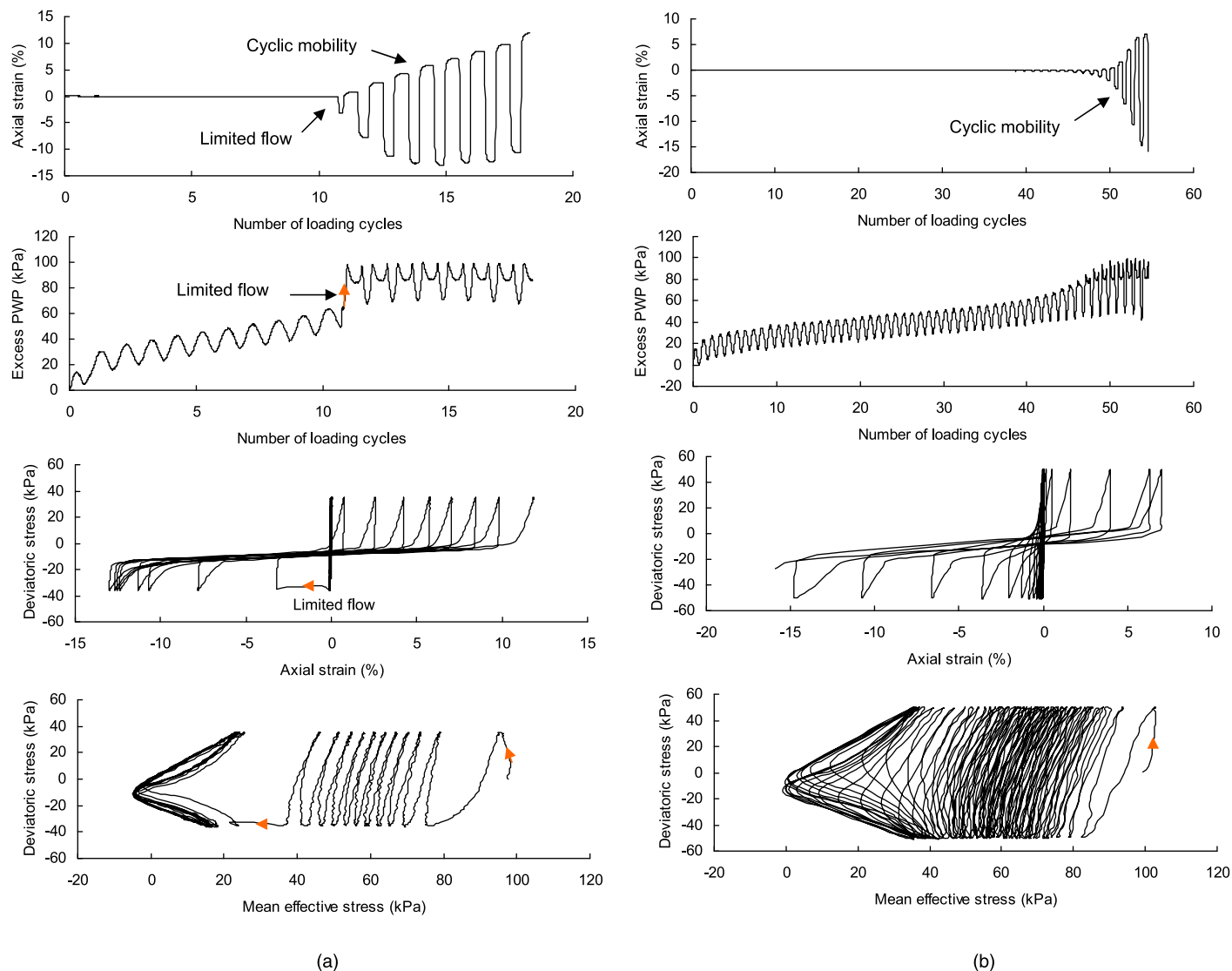
Fig. 5. Undrained response of medium-dense specimens as a result of cyclic loading without presence of initial static shear ($D_{rc} = 50\%$, $\sigma'_{nc} = 100$ kPa, $\alpha = 0$): (a) DD specimen; (b) MT specimen

deformation occurring in the 6th cycle and then being followed by a cyclic-mobility pattern. Compared with the test shown in Fig. 5(a), the abrupt deformation of the DD specimen was more severe ($\sim9\%$ axial strain), and the flow feature was more evident in the stress-strain curve and the stress path [Fig. 6(a)]. The observed difference in the degree of flow deformation is reasonable because the specimen shown in Fig. 6(a) was consolidated at a higher confining stress, thus leading to a more contractive response.

Keeping in mind the observed α-dependence of the effect of sample preparation on loose samples (Figs. 2–4), it is interesting to explore whether a similar difference exists for medium-dense specimens. Results of the tests for this purpose are shown in Fig. 7, where both specimens were anisotropically consolidated to an initial shear-stress level of $\alpha = 0.4$. Apparently, the response characteristics of the two specimens are quite similar regardless of the sample preparation method used. Both displayed the response that was typical of the mode known as plastic-strain accumulation (Yang and Sze 2011a), characterized by a pronounced axial strain in the first loading cycle and a continuous strain accumulation at an almost constant rate in the subsequent loading cycles. It is

noteworthy that in both cases the PWP built up in a progressive manner, and after several tens of cycles of loading, it was still far below the initial effective confining stress, implying that pore pressure generation is not a dominant factor for this failure mode.

Effect on Behavior of Dense Samples

Fig. 8(a) shows the response of a DD specimen at $D_{rc} = 70\%$ and $\sigma'_{nc} = 100$ kPa to symmetrically cyclic loading ($\alpha = 0$). The response of an MT specimen tested under similar conditions is shown in Fig. 8(b). Clearly, both specimens exhibited the cyclic-mobility pattern no matter which reconstitution method was used, implying that the effect is insignificant for dense samples. This observation was also found to hold true in the case of anisotropic consolidation (i.e., nonsymmetrical cyclic-loading conditions). In such a case, the deformation pattern known as plastic-strain accumulation, similar to that shown in Fig. 7, was dominant. For the sake of conciseness, the results of these tests are not presented here. It should be mentioned that while sample preparation appears to have a minor effect on dense sand in terms of deformation pattern and failure mechanism, it
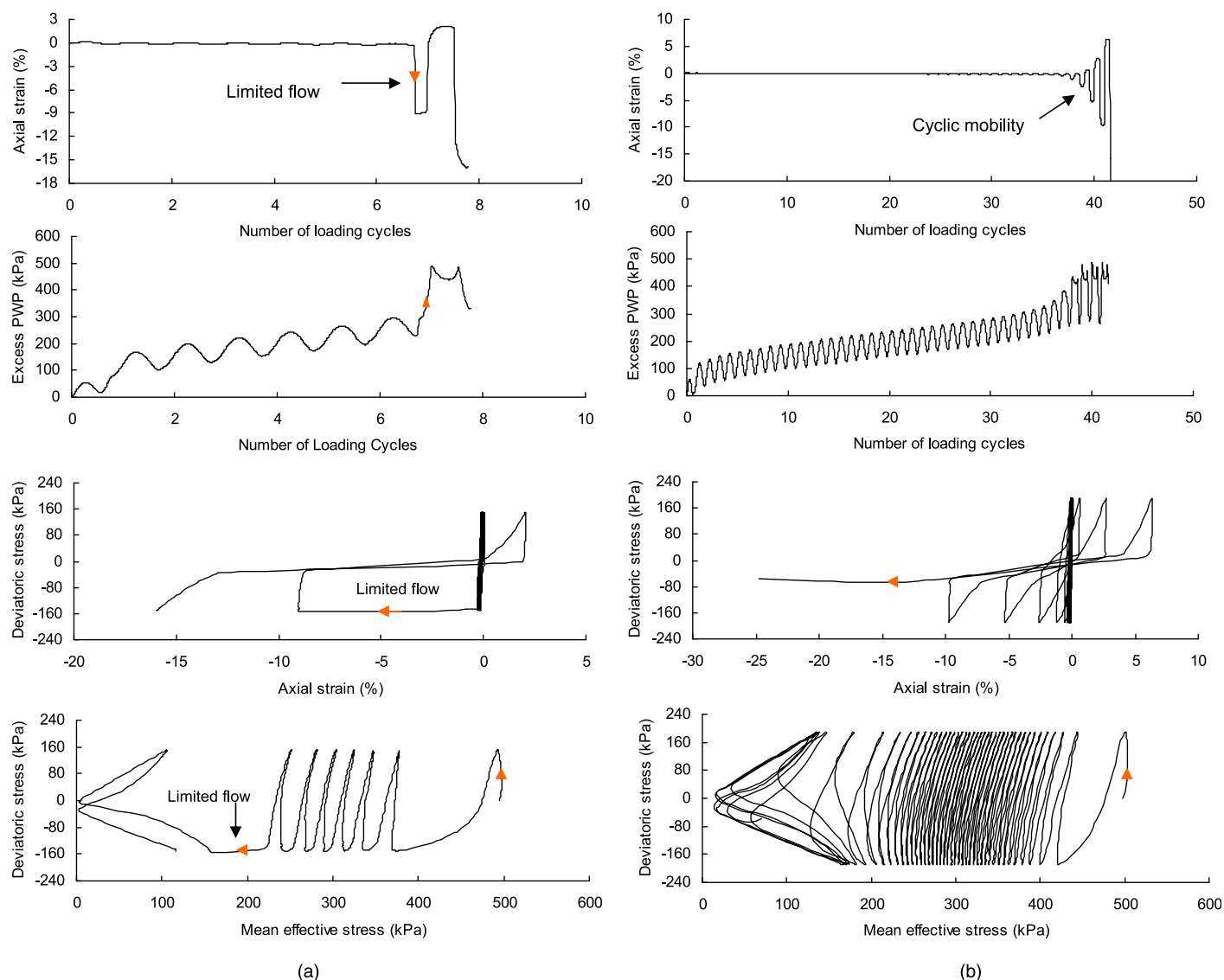
Fig. 6. Undrained response of medium-dense specimens as a result of cyclic loading without presence of initial static shear ($D_{rc} = 50\%$, $\sigma'_{nc} = 500$ kPa, $\alpha = 0$): (a) DD specimen; (b) MT specimen

had a marked effect on cyclic strength. A detailed discussion on this point will be given in the next section.

Summary of Observed Failure Modes

A thorough examination of the large number of tests conducted reveals that the deformation patterns generally can be categorized into five major types, as illustrated schematically in Fig. 9. The first three types, referred to as flow-type failure, cyclic mobility, and plastic-strain accumulation, have been observed repeatedly in MT specimens. The first type is pertinent to sufficiently loose samples with a contractive nature regardless of the presence or absence of an initial static shear stress, whereas medium-dense to dense samples exhibit either the mode of cyclic mobility or the mode of plastic-strain accumulation depending on the degree of stress reversal. Samples prepared by DD also can display these failure modes under certain conditions, as evidenced by the tests shown in Figs. 2, 7, and 8.

The other two failure modes shown in Fig. 9 were, however, observed exclusively in DD specimens. At a medium-dense state

with sufficient stress reversal in cyclic loading, the dominant failure mode was found to be the one shown in Fig. 9(d), referred to herein as limited flow followed by cyclic mobility. At a loose state without (or with slight) stress reversal in cyclic loading, the deformation pattern would be dominated by the one shown in Fig. 9(e), referred to as limited flow followed by strain accumulation.

Correspondence between Cyclic and Monotonic Sand Behavior

The cyclic-loading response has been found to be strongly linked with the monotonic-loading response under both isotropic (Alarcon-Guzman et al. 1988) and anisotropic (Yang and Sze 2011b) consolidation conditions. An interesting concern arising in this context is how the observed cyclic failure patterns, in particular, the limited-flow pattern, are related to the respective monotonic responses for specimens formed by different methods. To address this concern, a number of strain-controlled monotonic tests were conducted with special reference to the cyclic tests in the program. Several typical
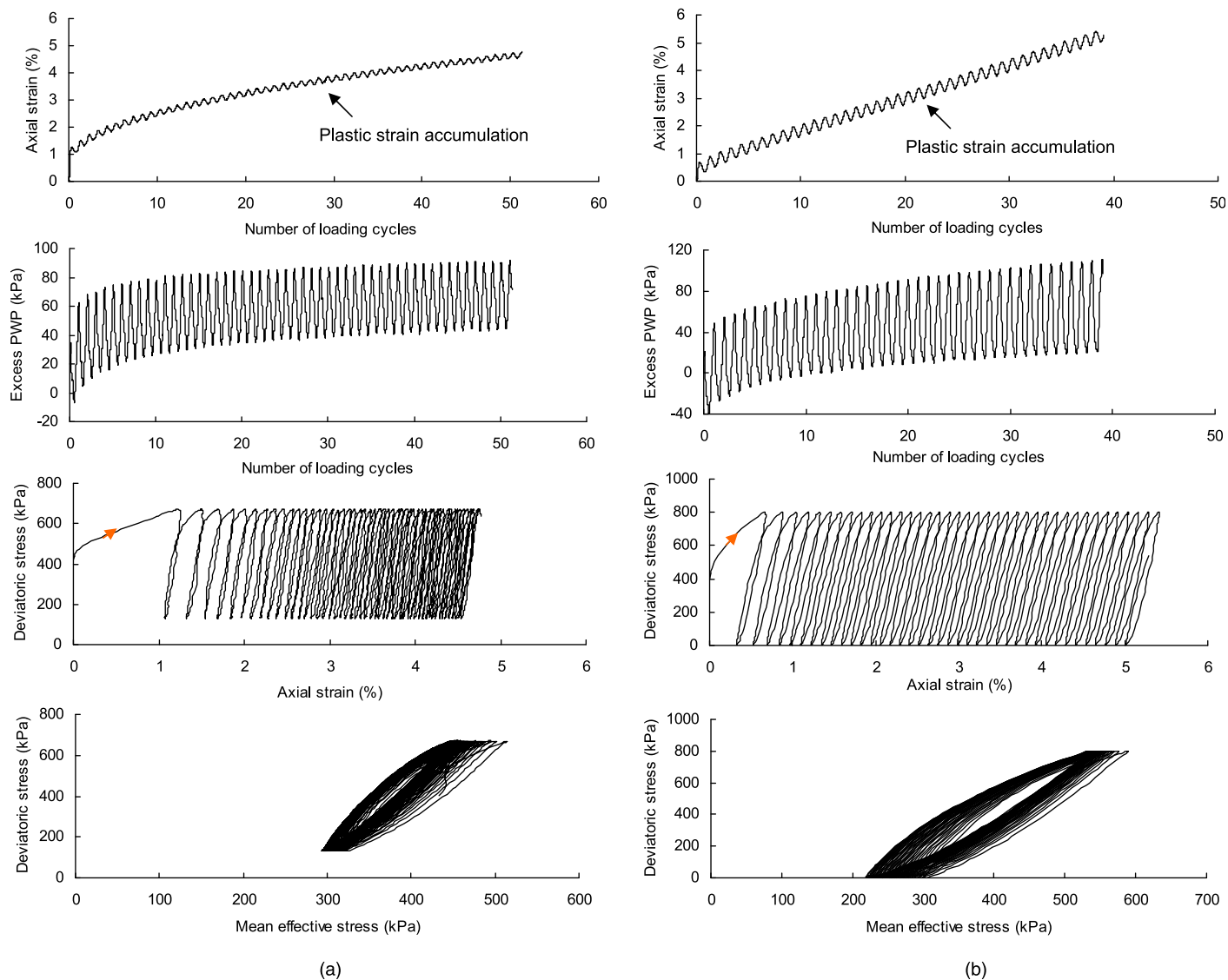
Fig. 7. Undrained response of medium-dense specimens as a result of cyclic loading with presence of initial static shear ($D_{rc} = 50\%$, $\sigma'_{nc} = 500\,\text{kPa}$, $\alpha = 0.4$): (a) DD specimen; (b) MT specimen

results are discussed here. Fig. 10 shows results of triaxial compression tests on two specimens prepared using MT and DD, respectively. Both were consolidated to the same density ($D_{rc} = 20\%$) and confining stress ($\sigma'_{nc} = 500\,\text{kPa}$).

The impact of the specimen preparation method or the fabric effect is evident. Whereas the MT specimen behaved in a highly contractive manner, the DD specimen exhibited a contractive response in the initial stage of shear that was then followed by a dilative, strain-hardening response to large deformation. Compared with the cyclic responses of the MT and DD specimens at a similar density and confining stress (see Fig. 3), the limited-flow response exhibited by the DD specimen in cyclic loading becomes reasonable. The triggering of flow was related to the occurrence of strain softening, but the flow was limited because of the associated strain-hardening response in the subsequent shear. On the other hand, because there was no such hardening response in the MT specimen in monotonic loading, the cyclic-loading test resulted in complete flow failure. More details about the link between cyclic- and monotonic-loading behavior is beyond the scope of this paper and will be presented elsewhere.

Failure Criteria, Cyclic Strength, and Fabric

Cyclic strength is an important design consideration in the evaluation of liquefaction potential. The common practice to determine cyclic strength from laboratory triaxial tests is to express the cyclic-stress ratio CSR_n defined in Eq. (3) as a function of the number of loading cycles to failure. In doing this, specification of the failure criterion is critical because it is from this that the number of cycles to cause failure is estimated. The conventional failure criterion is based on a certain level of double-amplitude strains or pore-water pressures (e.g., Mulilis et al. 1977; Tatsuoka et al. 1986a; Yamashita and Toki 1993). As will be shown later, this criterion would not be appropriate in certain situations.

Selection of Failure Criteria

For the first three failure modes shown in Fig. 9, namely, flow-type, cyclic mobility, and plastic-strain accumulation, it is rational to define failure, respectively, as the triggering of flow failure, the attainment of 5% axial strain in double amplitude (5% DA), and the
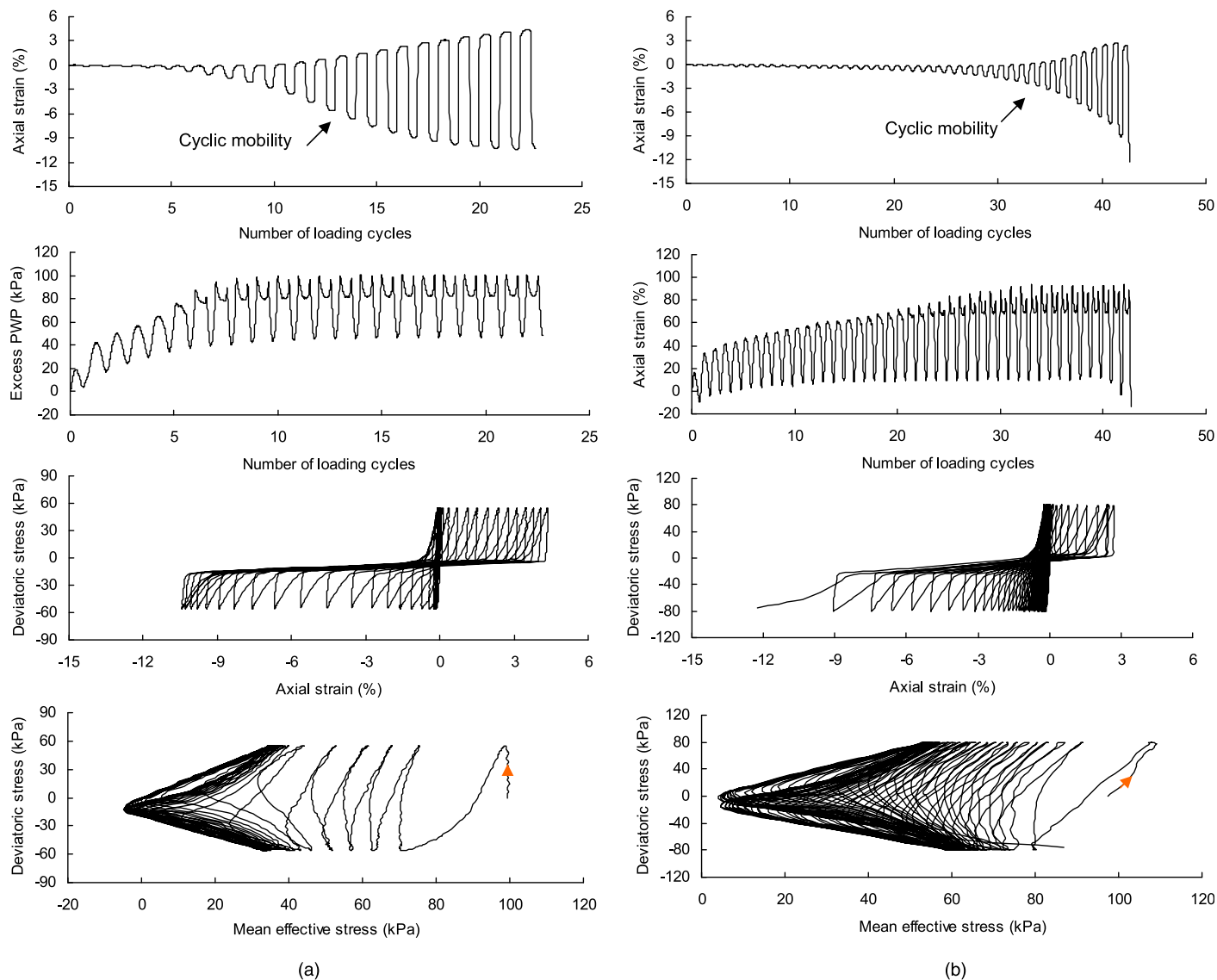
Fig. 8. Undrained response of dense sand specimens as a result of cyclic loading without presence of initial static shear ($D_{rc} = 70\%$, $\sigma'_{nc} = 100$ kPa, $\alpha = 0$): (a) DD specimen; (b) MT specimen

attainment of 5% peak axial strain in single amplitude (5% PS). For the two new failure modes in Figs. 9(d–e), their hybrid nature complicates the problem and requires careful examination.

First, referring to the mode defined as limited flow followed by plastic strain [Fig. 9(e)], it appears reasonable to regard failure as the abrupt onset of deformations for the following reasons: (1) The strain development at this instant is of a sudden nature, making it hard to predict; (2) although it is not excessive, the strain level developed at this instant still can be as large as 2%; and (3) the occurrence of the sudden deformation is always associated with a sudden rise in PWP or, correspondingly, a sudden drop of effective stress, as observed in Figs. 3(a) and 4(a). Despite these observations, one can observe that in this failure mode the sand can have itself stabilized after the limited flow in the form of progressive strain accumulation; in this connection, a certain level of residual strain (say 5%) may also be thought to be an acceptable failure criterion.

Similar considerations exist for the mode defined as limited flow followed by cyclic mobility, except that the residual strain accordingly should be defined as 5% in double amplitude [Fig. 9(d)]. Given these observations, it is necessary to examine the

consequence of different failure criteria on the evaluation of liquefaction resistance.

Effect of Failure Criteria on Cyclic Strength

Fig. 11(a) shows the values of CSR_n as a function of the number of loading cycles to failure for loose samples formed by DD at $D_{rc} = 20\%$, $\sigma'_{nc} = 100$ kPa, and $\alpha = 0.15$. Two cyclic strength curves resulted from using the two different failure criteria, as described previously. Similarly, two different cyclic strength curves were obtained for samples formed by DD at $D_{rc} = 35\%$, $\sigma'_{nc} = 500$ kPa, and $\alpha = 0.25$, as shown in Fig. 11(b). The substantial difference in the determined cyclic strength in both cases is striking, with the cyclic strength estimated using the strain-based criterion being markedly higher than that using the onset of limited flow as the failure criterion. Also, the degree of difference is found to depend on the number of cycles.

To better characterize the liquefaction resistance of sand, a CRR_n defined as the cyclic-stress ratio required causing failure at 10 loading cycles is introduced. The test results were interpreted to give CRR_n values at different densities and mean confining stresses as a
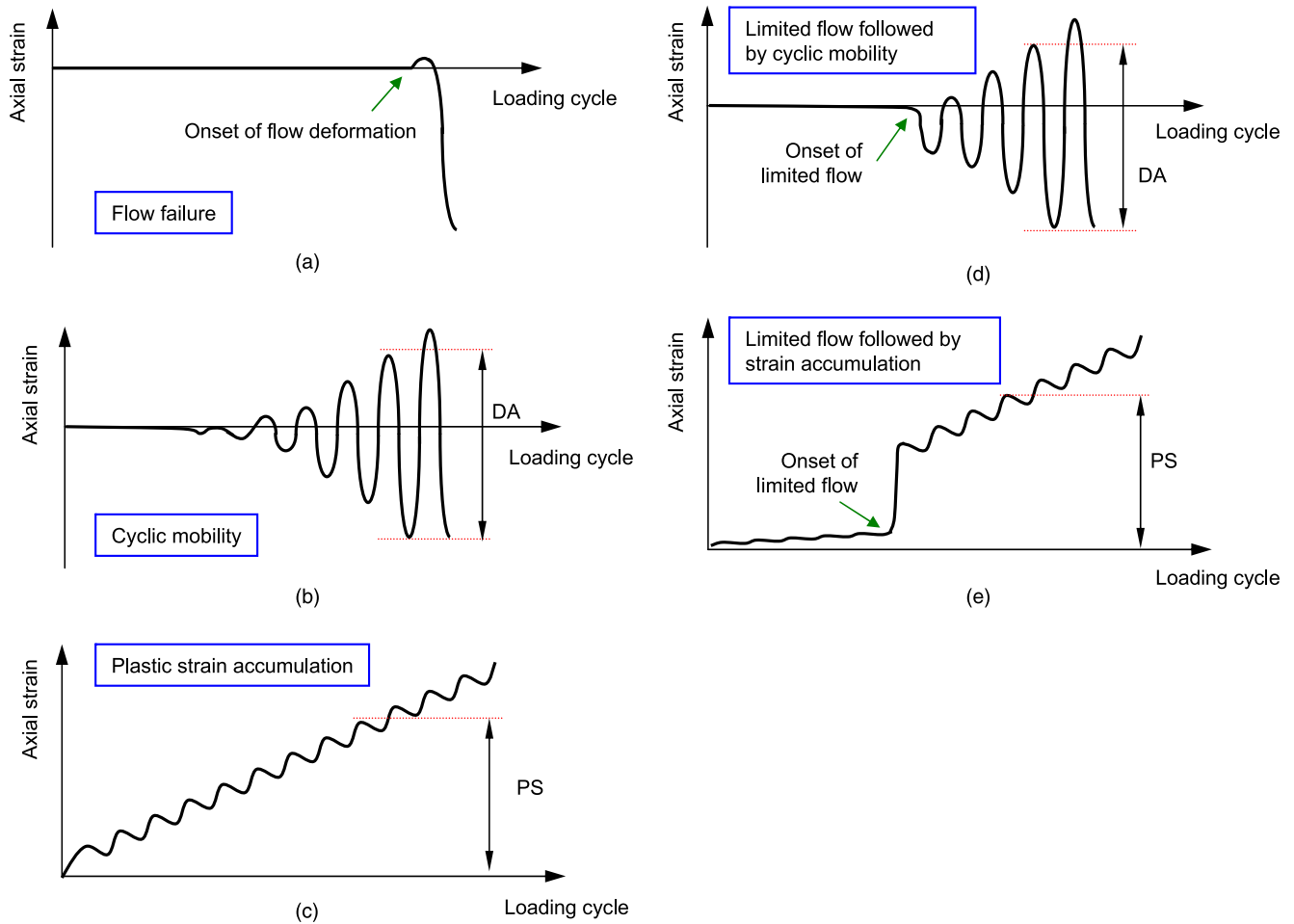
Fig. 9. Observed deformation patterns and failure mechanisms: (a) flow failure; (b) cyclic mobility; (c) plastic-strain accumulation; (d) limited flow followed by cyclic mobility; (e) limited flow followed by strain accumulation
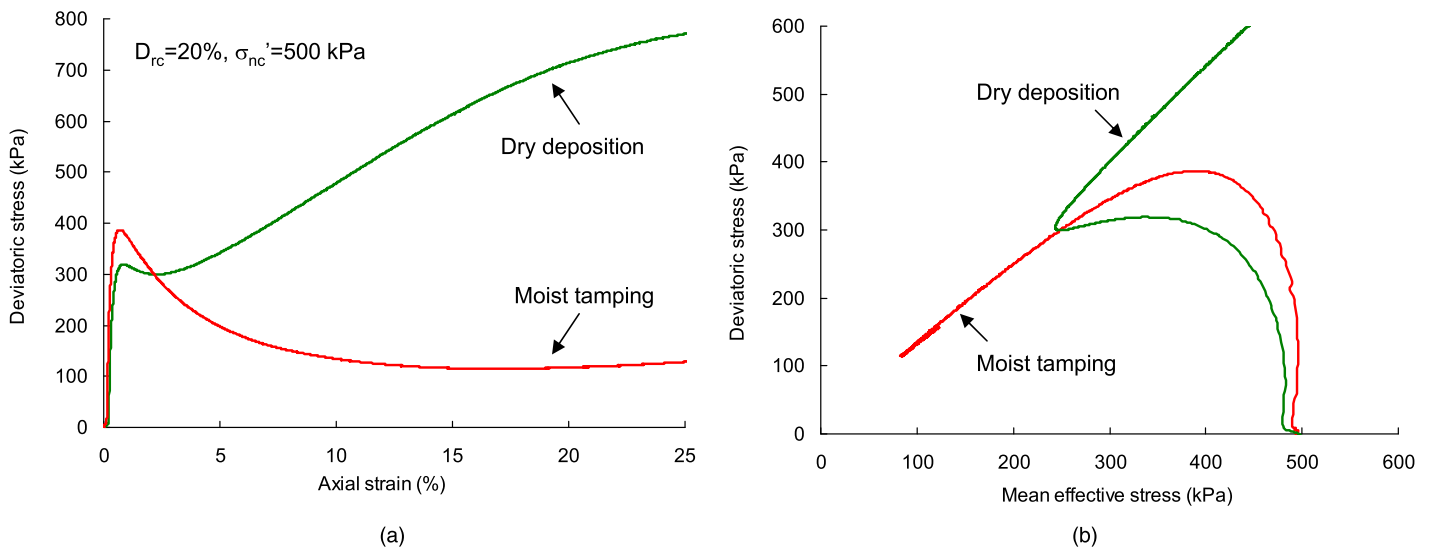

Fig. 10. Effect of sample preparation on undrained response of sand under monotonic loading: (a) stress-strain behavior; (b) stress path
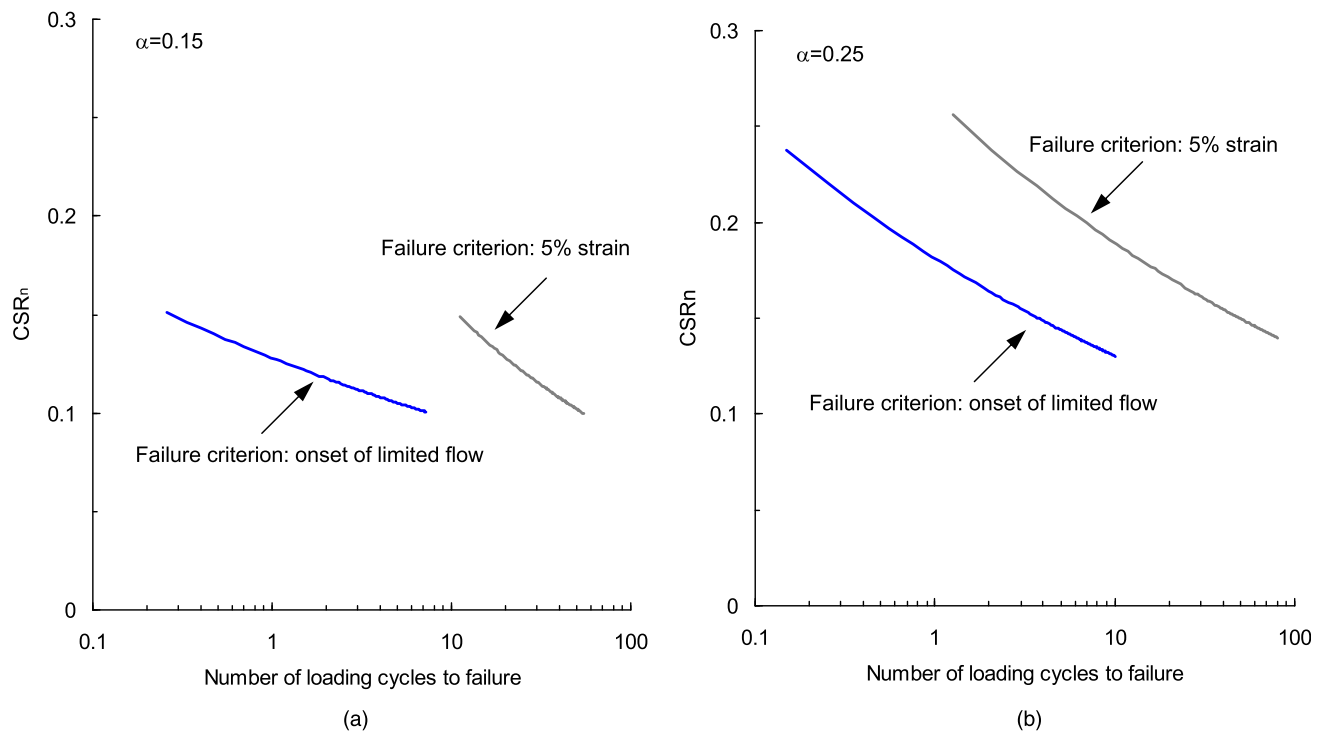
Fig. 11. Cyclic-stress ratio versus number of loading cycles to failure for DD specimens: (a) $D_{rc} = 20\%$, $\sigma'_{nc} = 100\,\text{kPa}$; (b) $D_{rc} = 35\%$, $\sigma'_{nc} = 500\,\text{kPa}$
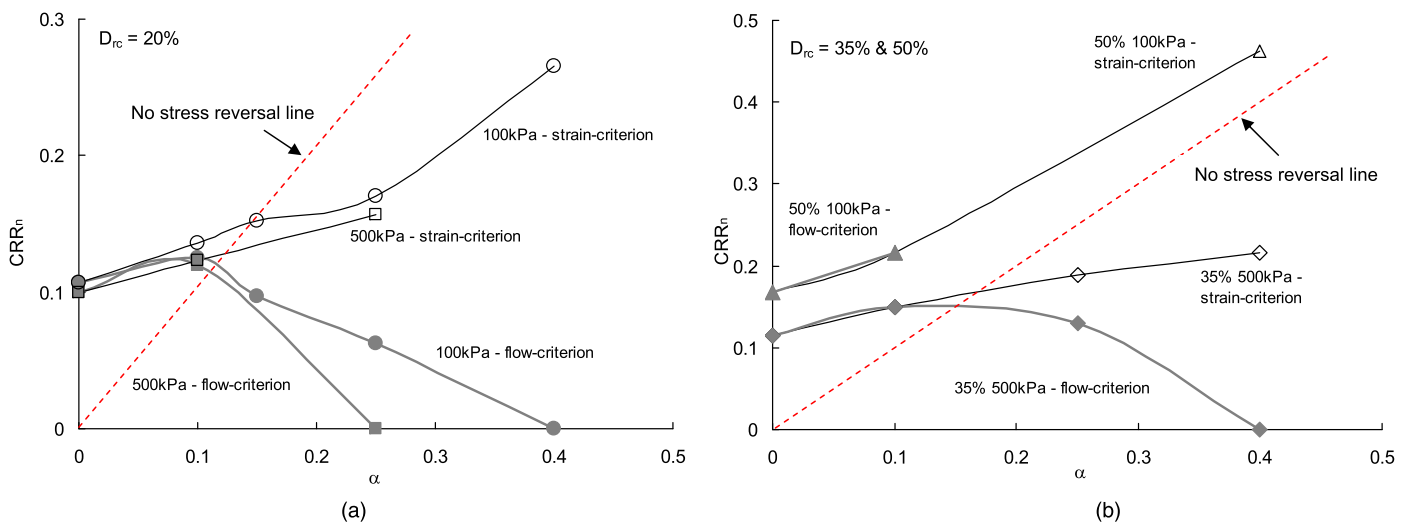

Fig. 12. Influence of failure criterion on relationship between cyclic strength and initial shear-stress level for DD specimens: (a) $D_{rc} = 20\%$; (b) $D_{rc} = 35$ and 50%

function of the initial shear-stress level α, as shown in Fig. 12(a) for samples of $D_{rc} = 20\%$ and in Fig. 12(b) for samples of $D_{rc} = 35$ and 50%. In producing the plots, the two failure criteria (i.e., 5% residual strain and the onset of limited flow) were adopted. Several key observations can be made from these results.

1. The selection of failure criterion has an effect not only on the interpreted cyclic strength but also on the α-dependence of cyclic strength;
2. This effect is marked on sand samples at loose state but tends to become less significant when sand samples become denser;

3. The strain-based criterion always results in higher CRR_n values and gives an increasing trend of CRR_n with α; and
4. The criterion based on the onset of limited flow gives lower CRR_n values and an increasing and then decreasing trend of CRR_n values with α.

Note that the increase and then decrease in CRR_n values with α are consistent with the concept of threshold α proposed by Yang and Sze (2011a) based on tests on MT samples. In line with this concept, a no-stress-reversal line has been drawn on each of the plots in Fig. 12, leading to the observation that CRR_n-α trend lines have their peaks at approximately the intersection points. Here a striking finding

JOURNAL OF GEOTECHNICAL AND GEOENVIRONMENTAL ENGINEERING © ASCE / JANUARY 2014 / **163**

J. Geotech. Geoenviron. Eng. 2014.140:152-169.

is that as long as the onset of limited flow is adopted as the failure criterion, the threshold-α concept becomes valid regardless of the sample preparation method used. However, if the strain-based criterion is used, the existence of a threshold α cannot be observed.

From the preceding discussion it becomes clear that the onset of limited flow is a more rational failure criterion for the hybrid failure modes. This criterion is also consistent with that set out for the flow-type failure mode, which shares similar mechanics with the limited-flow modes.

Effect of Reconstitution Method on Cyclic Strength

Having established a set of rational and consistent failure criteria, the relationship between the CSR_n and the number of loading cycles to failure was then determined for both DD and MT specimens. The two plots shown in Figs. 13(a and b) are cyclic-strength curves for loose specimens at $D_{rc} = 20\%$ and $\sigma'_{nc} = 100$ kPa, with and without the presence of an initial static shear stress ($\alpha = 0$ and 0.1). Similarly, Figs. 13(c and d) present cyclic-strength curves for medium

dense specimens at $D_{rc} = 50\%$ and $\sigma'_{nc} = 100$ kPa with and without the presence of an initial shear stress ($\alpha = 0$ and 0.1). Several important observations can be made from the plots.

1. The cyclic-strength curve determined from the tests on MT specimens is always located above the cyclic-strength curve determined for DD specimens regardless of the presence or absence of initial shear stress; and

2. The CSR_n values at 10 loading cycles (i.e., CRR_n values) for the MT samples are largely increased compared with the values for their DD counterparts, and the degree of difference depends on the initial shear-stress level and the state in terms of relative density and confining stress.

The result that MT samples have higher CSR_n values causing failure is consistent with previous studies for the symmetrical cyclic loading condition (Mulilis et al. 1977; Tatsuoka et al. 1986a); it is now extended to the nonsymmetrical loading condition (i.e., in the presence of initial static shear stress $\alpha \neq 0$) and to a much wider range of relative densities and confining stresses. To have a better view, the test results are reinterpreted as shown in Fig. 14, where
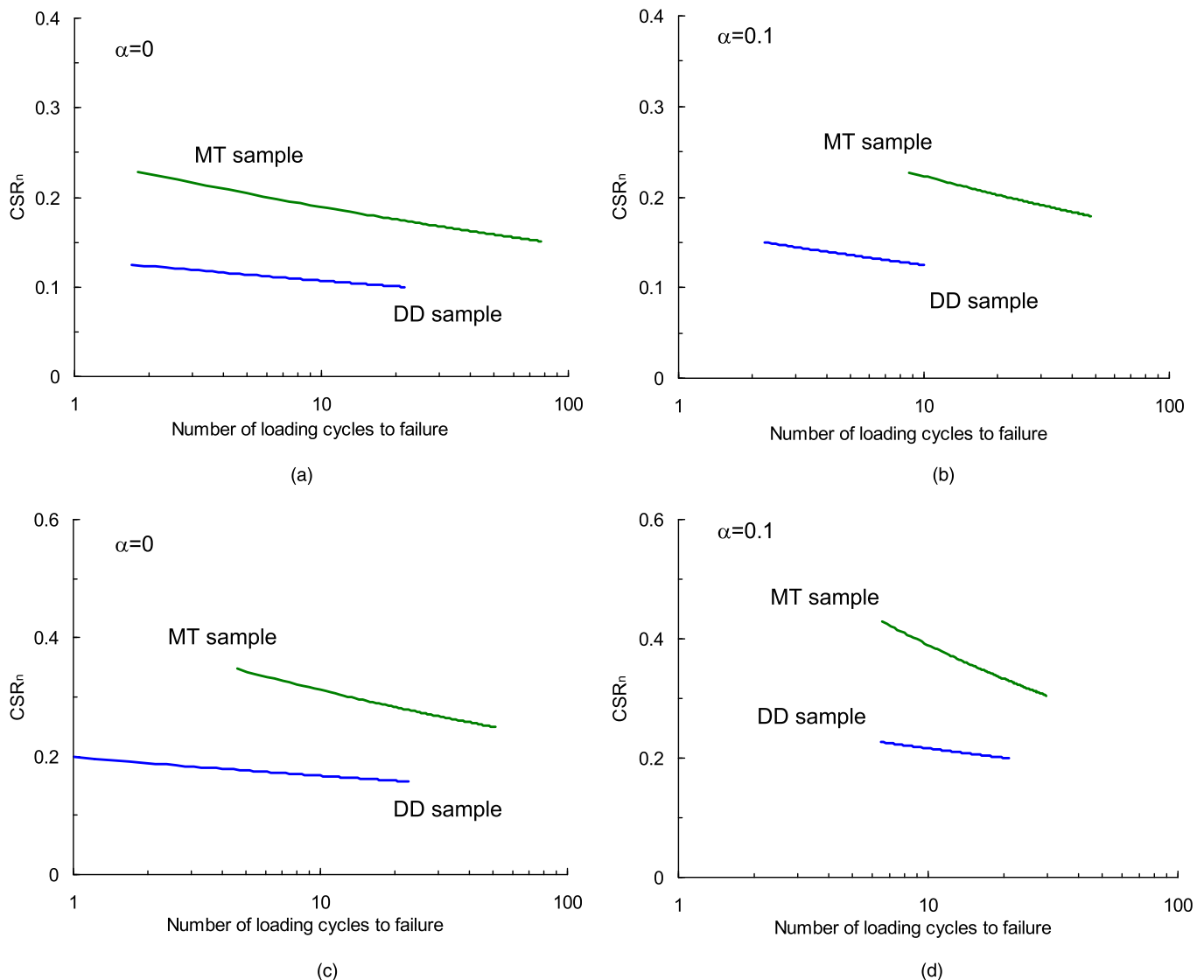

Fig. 13. Impact of sample preparation on relationship between cyclic-stress ratio and number of loading cycles to failure: (a and b) $D_{rc} = 20\%$, $\sigma'_{nc} = 100$ kPa; (c and d) $D_{rc} = 50\%$, $\sigma'_{nc} = 100$ kPa
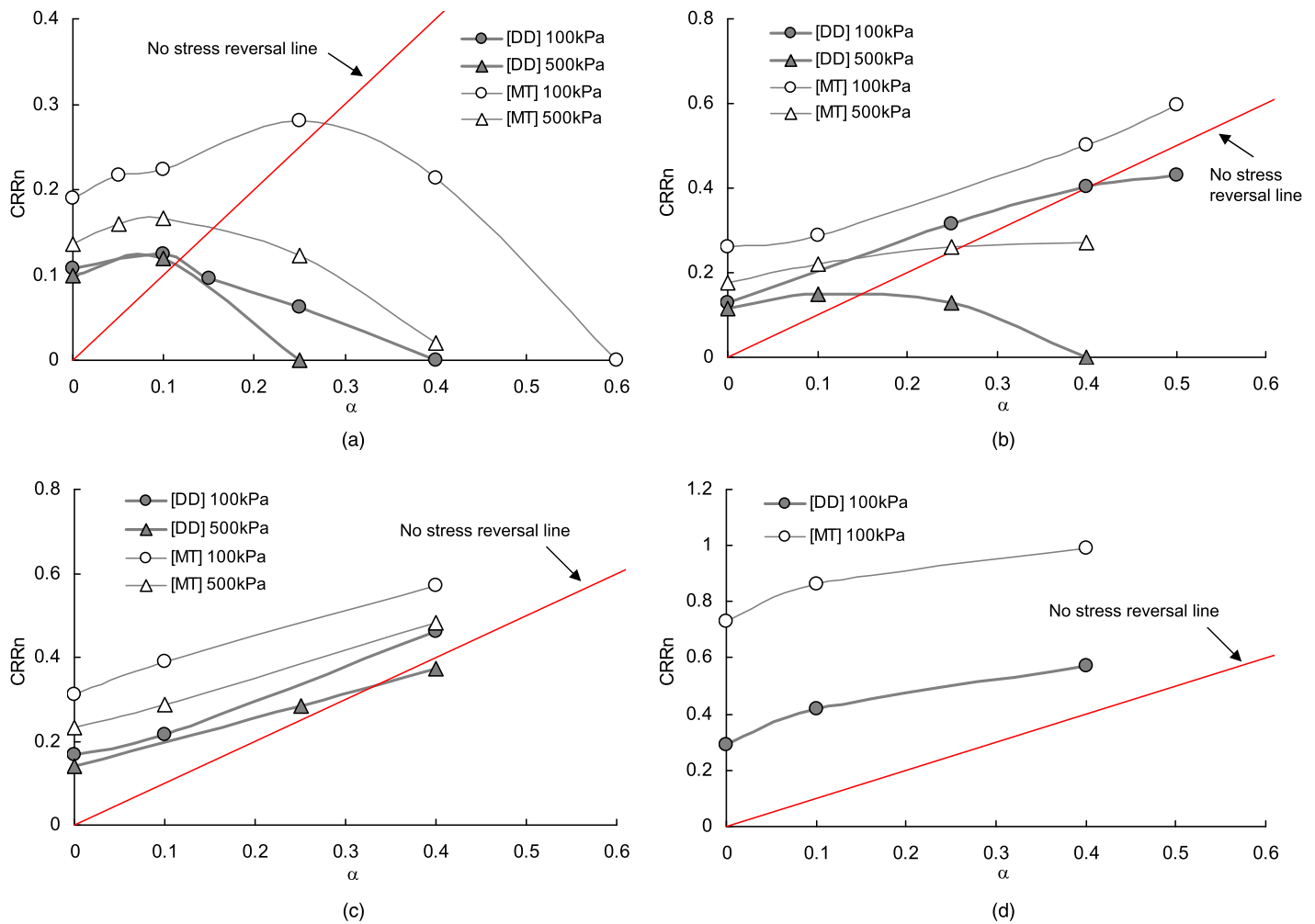
Fig. 14. Variation in cyclic strength with initial shear-stress level for DD and MT specimens: (a) $D_{rc} = 20\%$; (b) $D_{rc} = 35\%$; (c) $D_{rc} = 50\%$; (d) $D_{rc} = 70\%$
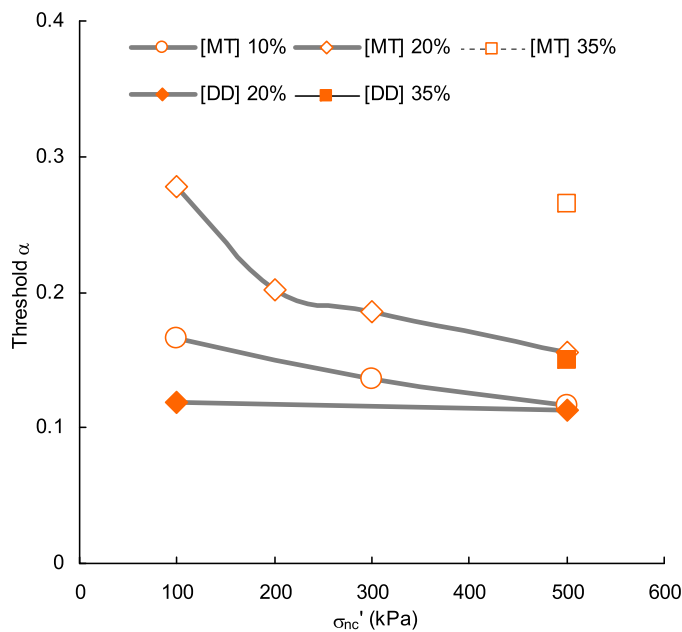

Fig. 15. Impact of sample preparation on threshold α

CRR_n values for MT and DD samples are presented as a function of α for different combinations of D_{rc} and σ'_{nc}. These plots provide clear evidence for the existence of threshold α and suggest that the value of threshold α depends on fabric, relative density, and confining stress.

An alternative view of the dependence of threshold α on these factors is given in Fig. 15, from which several marked features can be established.

1. The fabric formed by DD can largely reduce the threshold α level under otherwise similar conditions;
2. Given the same density, threshold α decreases as the mean confining stress increases for MT specimens, but this trend is not evident for DD specimens; and
3. Given the same reconstitution method and the same mean confining stress, threshold α increases with increasing density.

In the framework of critical-state soil mechanics, both cyclic strength and threshold α can be related to a state parameter that collectively accounts for relative density and confining stress, as elaborated by Yang and Sze (2011b) using the experimental data on MT specimens of Toyoura and Fujian sand. Within this new framework, a detailed analysis of the cyclic strength as affected by soil fabric is of interest. Given the scope of this paper and the limited space, the analysis will be reported in future papers.

JOURNAL OF GEOTECHNICAL AND GEOENVIRONMENTAL ENGINEERING © ASCE / JANUARY 2014 / **165**

J. Geotech. Geoenviron. Eng. 2014.140:152-169.

Particle-Scale Interpretations

The fabric of a sand specimen is basically a particle-scale property that can be described by the spatial orientation of particles or contact planes. Keeping this in mind, an attempt is made here to develop interpretations for the various macroscopic observations from a particle-scale perspective.

Degree of Fabric Anisotropy

Dry sand, when deposited under gravity, will have the long axes of grains orientated primarily in the horizontal direction (Oda 1972; Arthur and Menzies 1972); this is so because the particles tend to deposit at the most stable position. Correspondingly, the contact normals tend to align along the direction of deposition (i.e., the vertical direction). The preferential orientations of the particles and contact normals feature a high degree of anisotropy in the specimens formed by DD. A schematic illustration of the soil fabric is given in Fig. 16(a).

On the contrary, the MT method tends to result in a more isotropic fabric. This is so because the initial moisture contributes a certain level of suction that holds particles together, and thus the orientations of individual grains are not controlled by gravity. As a result, the MT specimens do not have a preferential particle orientation, leading to a lesser degree of anisotropy. The generally random particle orientation makes it a reasonable hypothesis that the fabric of MT specimens is likely to be in a honeycomb form (Casagrande 1975). Fig. 16(b) shows a schematic illustration of the fabric of MT specimens. Note that the illustrations in Fig. 16 are to highlight that MT specimens, compared with DD specimens, are

more isotropic. There is no intention to suggest that the fabric structure formed by MT is regular.

The considerations just described are supported by data from the imaging analysis of Yang et al. (2008) on the vertical sections of Toyoura sand specimens formed by MT and DD. By introducing a scalar quantity Δ known as the vector magnitude (Curray 1956; Oda and Iwashita 1999) to characterize the intensity of anisotropy of the particle orientation, the values of Δ were determined to be about 0.214 for DD specimens and 0.091 for MT specimens. Here $\Delta = 0$ represents perfect isotropy.

Change of Principal Stress Directions

Having accepted that DD specimens are more anisotropic and MT specimens are generally isotropic, the results that DD specimens were more susceptible to liquefaction failure in cyclic loading become understandable. As shown in Fig. 17, during cyclic loading that is symmetrical about the hydraulic stress axis, the direction of the major principal stress σ_1' will change by 90° in each loading cycle, from being triaxial compression to triaxial extension. When the major principal stress σ_1' is along the preferential orientation of the particles, the induced compressibility is much larger than that caused by the major principal stress acting in the deposition direction; in other words, the DD specimen is more contractive when σ_1' is perpendicular to the deposition direction (i.e., under extension loading). This has been evidenced by laboratory testing of the monotonic behavior of sand specimens with distinct fabrics (e.g., Oda 1972; Yang et al. 2008). In undrained cyclic tests, this means that the pace of PWP generation will be faster in a DD specimen than in an MT specimen, thus leading to higher liquefaction potential.
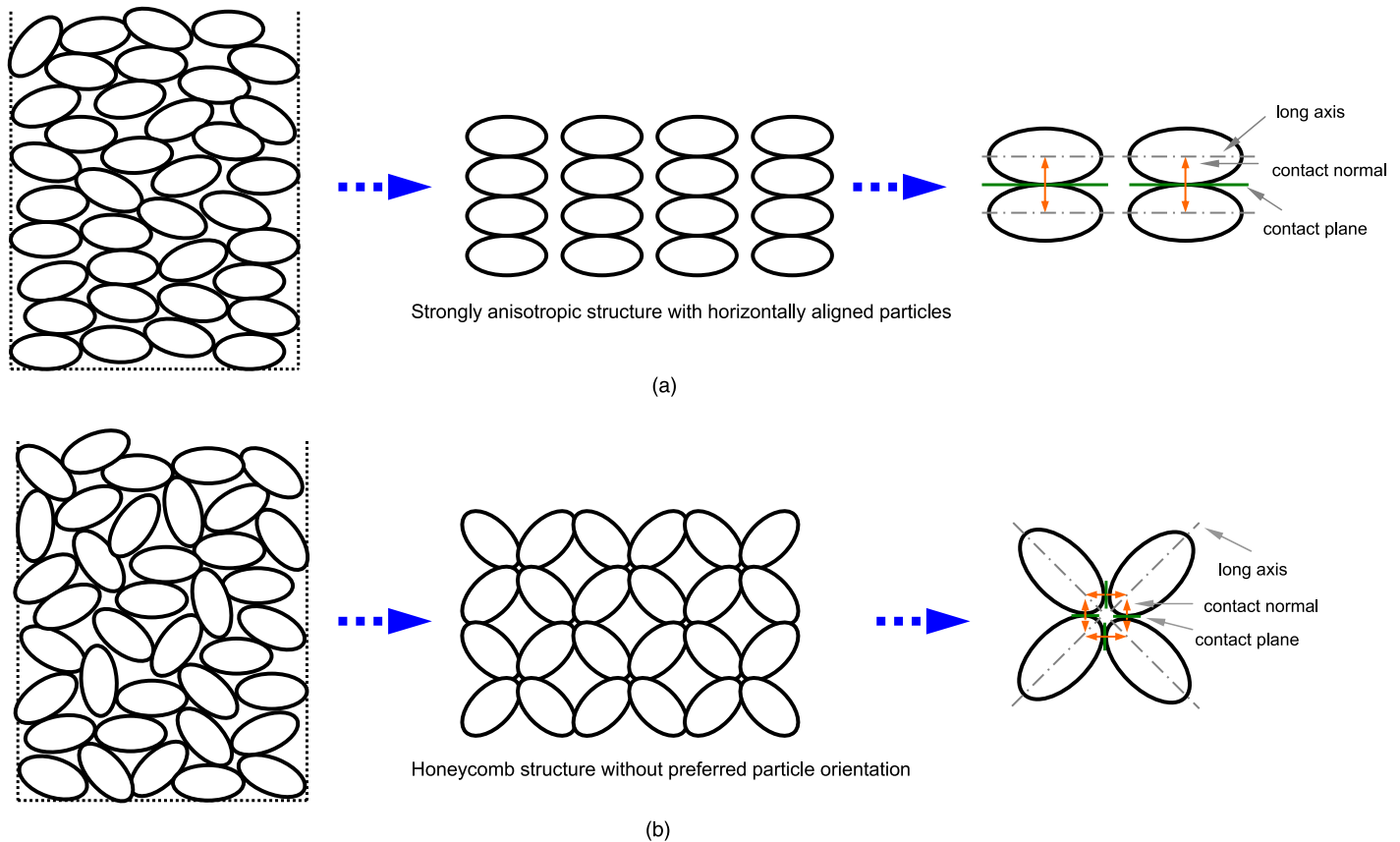

Fig. 16. Schematic illustration of fabrics of sand specimens prepared by (a) dry deposition; (b) moist tamping
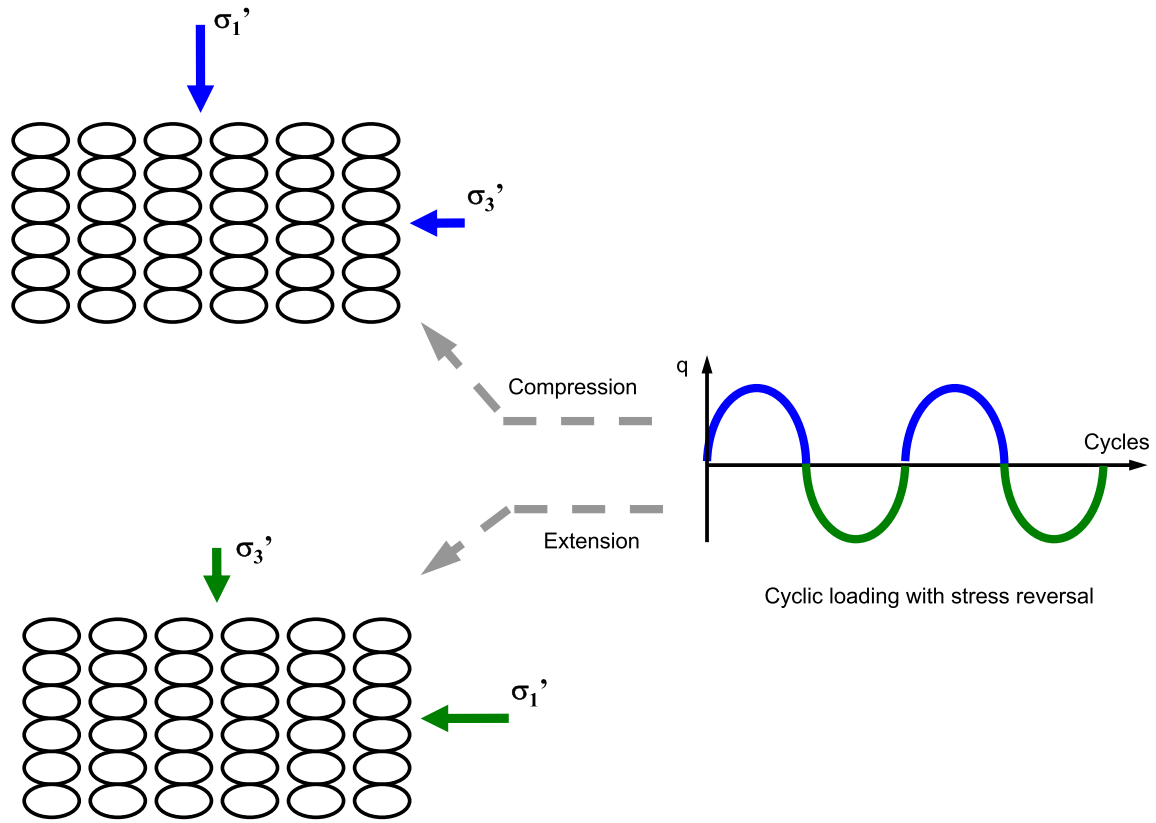
166 / JOURNAL OF GEOTECHNICAL AND GEOENVIRONMENTAL ENGINEERING © ASCE / JANUARY 2014

J. Geotech. Geoenviron. Eng. 2014.140:152-169.

Fig. 17. Schematic illustration of particle orientation and principal stress directions in DD specimen during cyclic loading with stress reversal
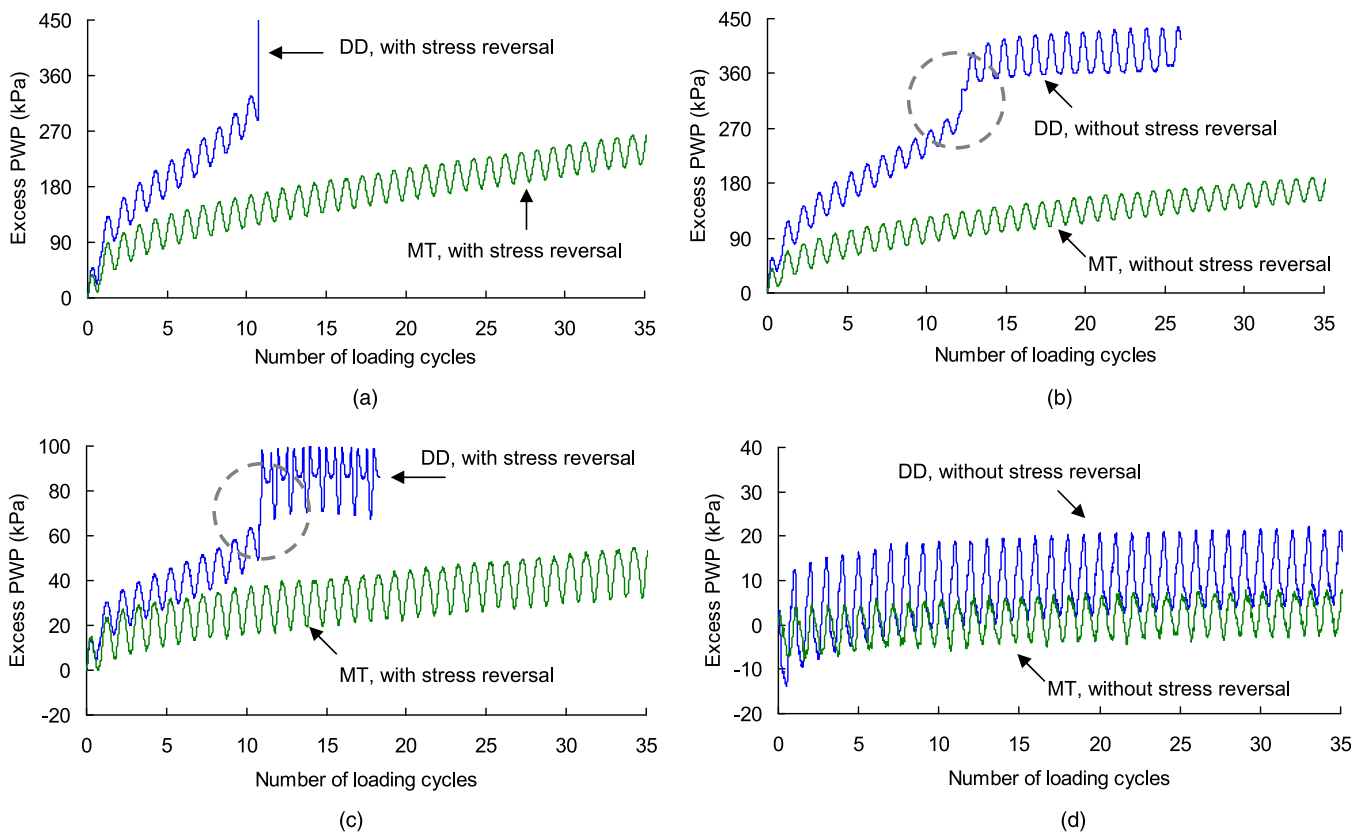

Fig. 18. Impact of sample preparation on pore-water-pressure buildup during cyclic loading: (a and b) loose state ($D_{rc} = 20\%$, $\sigma'_{nc} = 500\,\text{kPa}$); (c and d) medium-dense state ($D_{rc} = 50\%$, $\sigma'_{nc} = 100\,\text{kPa}$)

A close comparison of PWP data in the relevant cases (Fig. 18) offers good support to the idea.

When cyclic loading is nonsymmetrical without (or with slight) slight stress reversal, the degree of contractiveness of DD specimens tends to decrease because of a lack of extension loading compared with the symmetrical loading condition. This explains why the DD specimens exhibited the limited-flow pattern in the presence of an initial shear stress rather than a complete flow-type failure in the absence of the initial shear. The decrease in contractiveness resulting from a lack of stress reversal also results in a lower level of PWP; this is also supported by the PWP data shown in Fig. 18.

Summary and Conclusions

This paper presents an experimental study aimed at exploring the impact of sample preparation on the cyclic-loading behavior of saturated sand. The systematic data sets provide insights into the sand behavior under various cyclic-loading conditions and serve as a useful reference for the development of constitutive models tackling the effect of soil fabric. The significant findings of this study are summarized as follows:

1. Undrained cyclic deformation patterns can be categorized into five major types: flow-type failure, cyclic mobility, plastic-strain accumulation, limited flow followed by cyclic mobility, and limited flow followed by strain accumulation. The first three modes were observed in both MT and DD samples, whereas the other two were found exclusively in samples formed by DD.
2. The limited-flow modes are characterized by the abrupt onset of substantial yet limited deformations followed by a cyclic strain-hardening response. Their hybrid nature makes it crucial to define failure for liquefaction-resistance evaluation. The conventional failure criterion using a certain level of residual strain (e.g., 5%) does not appear to properly capture the failure mechanism involved, and it leads to higher estimates of liquefaction resistance than using the onset of limited flow as the criterion.
3. The concept of threshold α for nonsymmetrical loading conditions is valid regardless of the reconstitution method used so long as a rational failure criterion is used to quantify the cyclic strength. Threshold α depends on fabric, relative density, and confining stress. Under otherwise similar conditions, the fabric formed by DD can largely reduce the threshold-α level compared with the soil fabric formed by MT.
4. From the microscopic perspective, sand specimens formed by DD are highly anisotropic with a preferential orientation of the particles, whereas MT specimens are more isotropic. This difference in fabric anisotropy results in DD specimens being highly contractive when the major principal stress becomes normal to the deposition direction during cyclic loading, explaining why they have lower resistance to liquefaction and why their response is more sensitive to the degree of stress reversal.
5. The method of specimen preparation or the fabric it forms plays an important role in the nature of sand response to cyclic loading. The impact is not monotonic but rather depends on the density, confining stress, initial static shear stress, and degree of stress reversal during cyclic loading. The fabric should be regarded as a state parameter as important as the conventional ones (i.e., density and confining stress) in describing soil behavior.

Acknowledgments

Notation

The following symbols are used in this paper:

CRR_n = cyclic resistance ratio;
CSR_n = cyclic stress ratio;
D_{rc} = relative density after consolidation;
p' = mean effective stress;
q = deviatoric stress;
q_{cyc} = cyclic deviatoric stress;
q_s = initial static deviatoric stress;
Δ = vector magnitude describing degree of anisotropy;
α = initial static shear stress ratio;
σ'_{nc} = effective normal stress on 45° plane;
σ'_1 = effective major principal stress;
σ'_{1c} = effective major principal consolidation stress;
σ'_3 = effective minor principal stress; and
σ'_{3c} = effective minor principal consolidation stress.

References

Alarcon-Guzman, A., Leonards, G. A., and Chameau, J. L. (1988). "Undrained monotonic and cyclic strength of sands." *J. Geotech. Engrg.,* 114(10), 1089–1109.

Arthur, J. R. F., and Menzies, B. K. (1972). "Inherent anisotropy in a sand." *Geotechnique,* 22(1), 115–128.

Brewer, R. (1964). *Fabric and mineral analysis of soils*, Wiley, New York.

Casagrande, A. (1975). "Liquefaction and cyclic deformation of sands: A critical review." *Proc., 5th Pan-American Conf. on Soil Mechanics and Foundation Engineering.*, Vol. 5, 79–133.

Castro, G. (1975). "Liquefaction and cyclic mobility of saturated sands." *J. Geotech. Engrg. Div.,* 101(GT6), 551–569.

Curray, J. R. (1956). "The analysis of two-dimensional orientation data." *J. Geol.,* 64(2), 117–131.

Hyodo, M., Tanimizu, H., Yasufuku, N., and Murata, H. (1994). "Undrained cyclic and monotonic triaxial behaviour of saturated loose sand." *Soils Found.,* 34(1), 19–32.

Idriss, I. M., and Boulanger, R. W. (2008). *Soil liquefaction during earthquakes*, Earthquake Engineering Research Institute, Oakland, CA.

Ishihara, K. (1993). "Liquefaction and flow failure during earthquakes." *Geotechnique,* 43(3), 351–415.

Ladd, R. S. (1974). "Specimen preparation method and liquefaction of sands." *J. Geotech. Engrg. Div.*, 100(GT10), 1180–1184.

Miura, S., and Toki, S. (1982). "A sample preparation method and its effect on static and cyclic deformation strength properties of sand." *Soils Found.,* 22(1), 61–77.

Mohamad, R., and Dobry, R. (1986). "Undrained monotonic and cyclic strength of sand." *J. Geotech Engrg.,* 112(10), 941–958.

Mulilis, J. P., Seed, H. B., Chan, C. K., Mitchell, J. K., and Arulanandan, K. (1977). "Effects of sample preparation on sand liquefaction." *J. Geotech. Engrg. Div.,* 103(GT2), 91–108.

Oda, M. (1972). "Initial fabrics and their relations to mechanical properties of granular material." *Soils Found.,* 12(1), 17–35.

Oda, M., and Iwashita, K. (1999). *Mechanics of granular materials: an introduction*, Balkema, Rotterdam, Netherlands.

Peacock, W. H., and Seed, H. B. (1968). "Sand liquefaction under cyclic loading simple shear conditions." *J. Soil Mech. and Found. Div.,* 96(SM3), 689–708.

Seed, H. B. (1983). "Earthquake-resistant design of earth dams." *Proc., Symp. on Seismic Design of Earth Dams and Caverns*, ASCE, Reston, VA, 41–64.

Seed, H. B., and Lee, K. L. (1966). "Liquefaction of saturated sands during cyclic loading." *J. Soil Mech. and Found. Div.,* 92(6), 105–134.

Tatsuoka, F., et al. (1986b). "Some factors affecting cyclic undrained triaxial strength of sand." *Soils Found.*, 26(3), 99–116.

Tatsuoka, F., Ochi, K., Fujii, S., and Okamoto, M. (1986a). "Cyclic undrained triaxial and torsional shear strength of sands for different sample preparation methods." *Soils Found.*, 26(3), 23–41.

Vaid, Y. P., and Chern, J. C. (1983). "Effect of static shear on resistance to liquefaction." *Soils Found.*, 23(1), 47–60.

Vaid, Y. P., and Chern, J. C. (1985). "Cyclic and monotonic undrained response of saturated sands." *Proc., Advances in the Art of Testing Soils under Cyclic Loading Conditions,* ASCE, Reston, VA, 171–176.

Vaid, Y. P., Sivathayalan, S., and Stedman, D. (1999). "Influence of specimen reconstituting method on the undrained response of sand." *ASTM Geotech. Test. J.*, 22(3), 187–195.

Verdugo, R., and Ishihara, K. (1996). "The steady state of sandy soils." *Soils Found.*, 36(2), 81–91.

Wong, R. T., Seed, H. B., and Chan, C. K. (1975). "Cyclic loading liquefaction of gravelly soils." *J. Geotech. Engrg. Div.,* 101(GT6), 571–583.

Yamashita, S., and Toki, S. (1993). "Effects of fabric anisotropy of sand on cyclic undrained triaxial and torsional strengths." *Soils Found.*, 33(3), 92–104.

Yang, J., and Sze, H. Y. (2011a). "Cyclic behaviour and resistance of saturated sand under non-symmetrical loading conditions." *Geotechnique*, 61(1), 59–73.

Yang, J., and Sze, H. Y. (2011b). "Cyclic strength of sand under sustained shear stress." *J. Geotech. Geoenviron. Eng.,* 137(12), 1275–1285.

Yang, J., and Wei, L. M. (2012). "Collapse of loose sand with the addition of fines: The role of particle shape." *Geotechnique*, 62(12), 1111–1125.

Yang, Z. X., Li, X. S., and Yang, J. (2008). "Quantifying and modelling fabric anisotropy of granular soils." *Geotechnique*, 58(4), 237–248.